Data-driven methods in application to flood defence systems monitoring and analysis

Pyayt, A.L.

Publication date
2014

Chapter 6. Combination of Data-driven Methods and Physical Modelling*

The possible strategies of combination of data-driven methods with physical modelling are described in this chapter. Two examples of combination of the anomaly detection approach with physical modelling are presented.

6.1. Approach for combination

In this Section we summarize possible ways of communication of the anomaly detection approach based on data-driven methods (implemented within the Artificial Intelligence (AI) component – see Chapter 5) with the computational models providing physical simulation of behaviour of the monitored object.

A conceptual scheme of computer modelling (CM) component is presented in Figure 6.1. CM is a module that consists of the "Dike Mechanical Model" and the "Interpreter" blocks. First one is based on the method of finite element modelling and serves to imitate behaviour of a real dike under various environmental conditions. Second one is needed to translate the results of computational modelling into language known to the artificial intelligence (AI) component and experts. CM takes as the input information about environment and sensor data from a real dike. As the output it produces virtual sensor data and risk assessment.

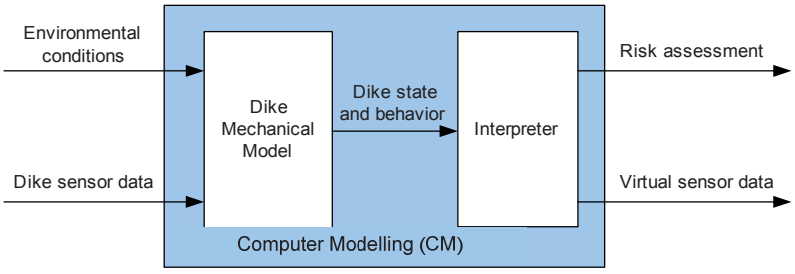

Figure 6.1. Computer modelling (CM) component.

Validation of the CM component serves to check a quality of its behaviour imitation. An idea of a validation process is presented in Figure 6.2. To examine the model quality, set of virtual and real sensor indications for the same environmental conditions have to be compared. The output of the "Comparator" element estimates the agreement between the CM imitation results and real dike data. Assume that a CM component describes behaviour

* Parts of this chapter were published in Pyayt, A.L., Mokhov, I.I., Kozionov, A., Kusherbaeva, V., Melnikova, N.B., Krzhizhanovskaya, V.V., Meijer, R.J. Artificial intelligence methods and finite element model application for on-line dike measurements processing. Proceedings of the 2011 IEEE Workshop on Environmental, Energy, and Structural Monitoring Systems (EESMS), Milan, Italy, 28 September 2011, pp 1-7, DOI: 10.1109/EESMS.2011.6067047

of a real dike with sufficient accuracy. Virtual sensor data produced by the computer model can be used to train an AI component.

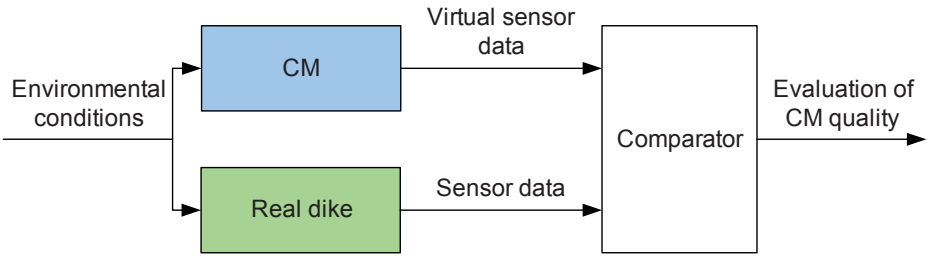

Figure 6.2. Validation of computer modelling component.

Procedure of training is presented in Figure 6.3. The input of CM model consumes a dataset of year-round historical and predicted environmental conditions. If modelling results show an absence of a risk for dike stability, virtual sensor data produced by the CM are used to train the AI component.

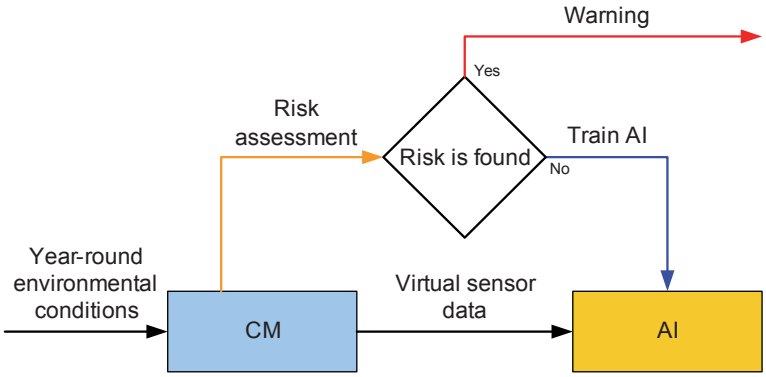

Figure 6.3. Training the artificial intelligence (AI) component using the virtual sensor data.

When the AI component detects an abnormal behaviour, the advanced computer models are launched. The CM starts calculations of a dike condition to assess whether current state is critical. If the modelling shows that situation is normal then current condition can be added to the set of "normal" states in the AI component (Figure 6.4).

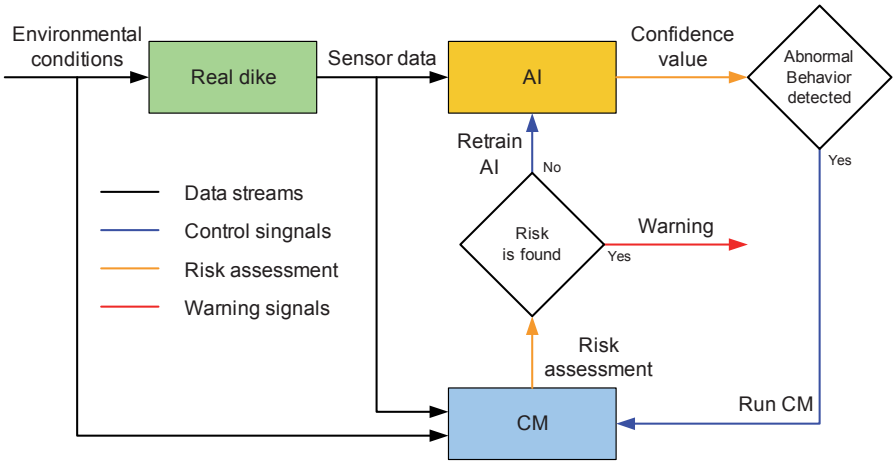

Figure 6.4. Combination of artificial intelligence (AI) and computer modelling (CM) components in one data processing chain.

The idea is to form a dataset, which would contain information on different kinds of dike failures (a breach, a piping, a slippage) (Figure 6.5). The dataset should be formed using measurements collected from a real dam or using results of modelling taking into account expert knowledge. The next step is training of the AI component in order to form a set of clusters for further recognition of various types of dike behaviour. As an output, this component will provide a set of confidence values for every specific predetermined class of failure and a general confidence value of levee behaviour.

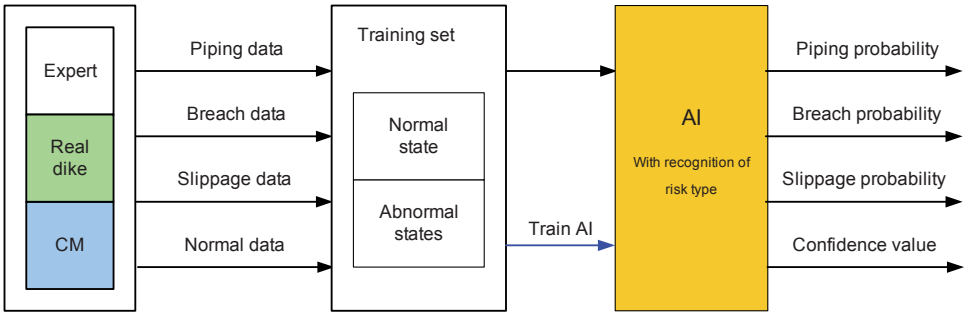

Figure 6.5. Preparation of the training set for the dam failure detection.

6.2. Combination within the UrbanFlood project

6.2.1. Virtual Dike

The *Virtual Dike* is a finite element model developed within the *UrbanFlood* project by the University of Amsterdam for simulation of levee behaviour [82], [80]. The finite element model was designed similar to the LiveDike – a sea dike protecting the port of

Groningen in the Netherlands (Figure 6.6(a)). LiveDike was equipped with 56 *GeoBeads* sensors installed in four cross-sections. More information about the levee can be found in [83].

The geometric configuration and boundary conditions of the model dike are similar to those of the LiveDike, while material properties have been artificially set weaker, to obtain a more pronounced plastic zone under the condition of a simulated flood. A model dike is composed of homogeneous sand. More details about the constructed model are presented in work [104].

In order to generate a training set for the AI component, an abnormal behaviour of the dike has been simulated. Flood condition has been modelled by linearly increasing the water level from a Mean Sea Level (MSL) to the artificially extremely high level of +6.6 m above the MSL. The top of the dike is at 9 m. In Figure 6.6(b) are presented locations of the six "virtual" sensors at the land-side slope of the dike where simulation results are probed for stability criterion.

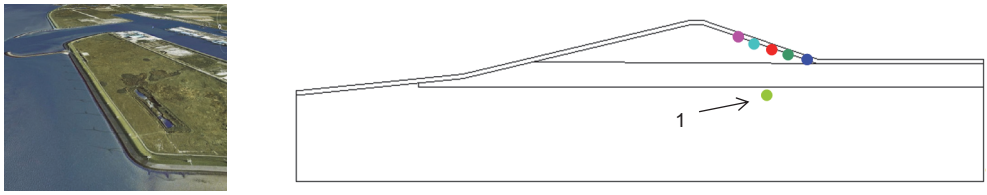

Figure 6.6. (**a**) Photo of LiveDike. (**b**) Locations of six "virtual" sensors where simulation results are probed for stresses and stability criterion [104].

Stability criterion dynamics is shown in Figure 6.7. Criterion values become negative with plastic deformations taking place.

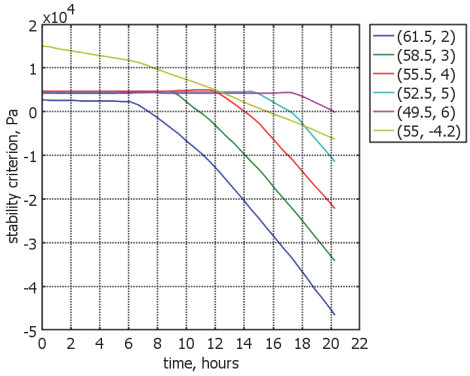

Figure 6.7. Stability criterion dynamics, for six virtual sensors located as shown in Figure 6.6(b) [104].

6.2.2. Detection of artificially generated anomaly

The first principal strain and X deformation measured by the virtual sensor located at point (X=55 m, Y=-4.2 m – green point marked with arrow in Figure 6.6(b)) were used as input parameters for the one-side classifier by Neural Clouds.

Figure 6.8 shows the constructed Neural Clouds for calculation of the confidence value of dike normal behaviour.

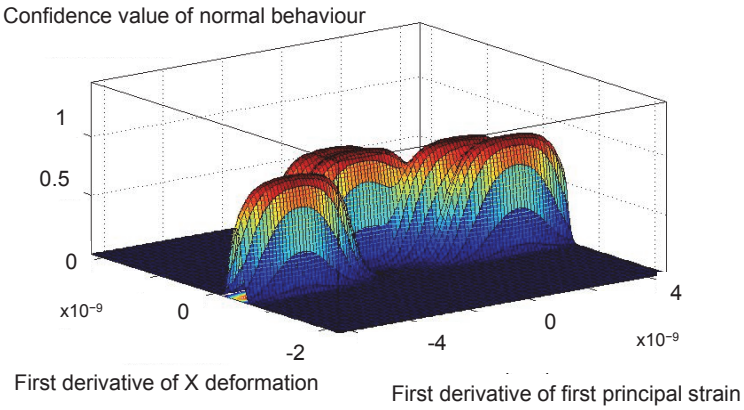

Figure 6.8. 3D view of the constructed Neural Clouds.

Figure 6.9 presents input variables (first principal strain and X deformation - (a) and (b) parts of figure) and time dynamics of the confidence value (c).

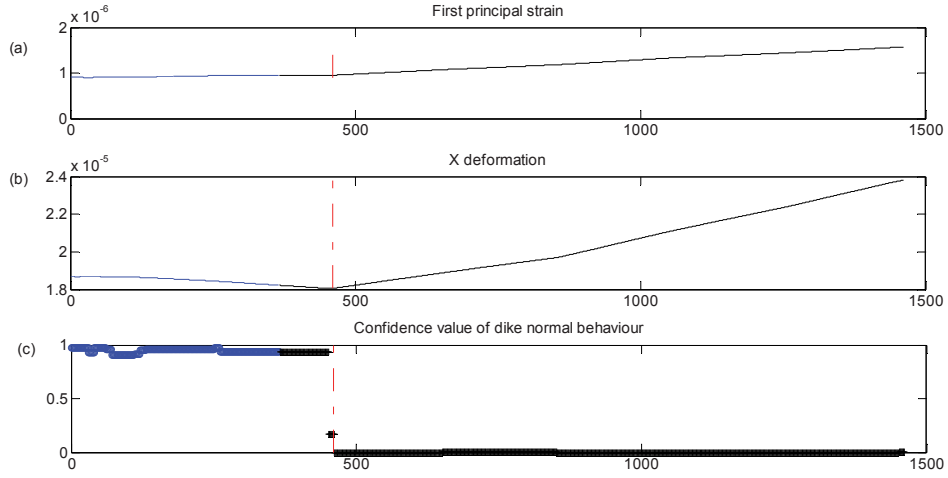

Figure 6.9. Detection of anomaly using the Neural Clouds (NC) approach. (**a**) and (**b**) represent the input data; (**c**) illustrate the calculated confidence values. Blue lines indicate the training period (timestamps 1-460), black lines indicate the testing period (timestamps 461 and further).

The first principal strain is a metric of maximal strain in soil skeleton. Intensive deformations in a dike always precede failure. The more intensive deformations occur in a dike, the higher these metrics are. X deformation here is the displacement of a material point in soil along X-axis. Naturally, rapidly developing displacements are markers of intensive sliding (which is a failure process) occurring in the dike.

Vertical red line in Figure 6.9 shows the moment when confidence value went down from the values close to 1 (normal behaviour) to zero (detected anomaly).

Figure 6.10 demonstrates the ability of Neural Clouds to detect anomaly: confidence value went down to zero at the moment when the stability factor changed the slope angle. The dike failure can occur when the stability factor becomes zero and lower. In Figure 6.10 it happens around the time step 1100, which means that the AI detected the onset of forthcoming dike instability over 600 time steps earlier [104].

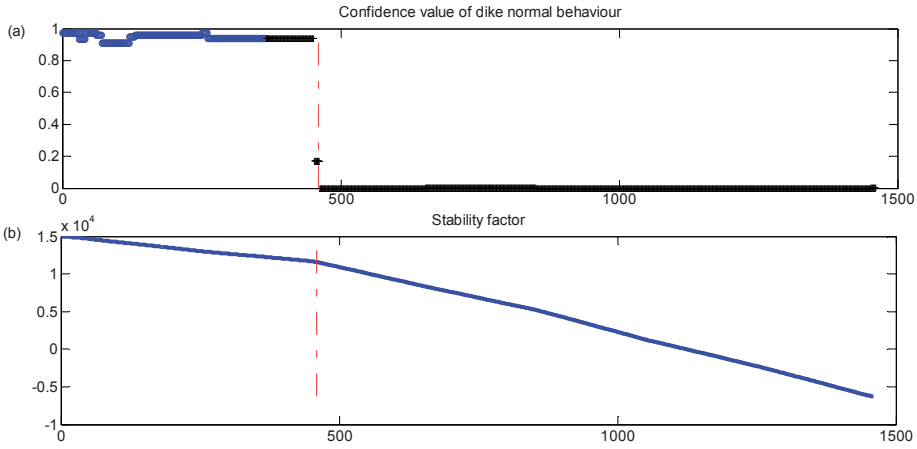

Figure 6.10. Detection of dike anomaly. (**a**) Confidence value of dike normal behaviour calculated by Artificial Intelligence (AI) component. Blue line is training period, black line is testing period. (**b**) Stability criterion calculated by the *Virtual Dike* finite element model.

6.3. Combination within the IJkdijk project

In this section we present results of combination with the physical model developed by Siemens LLC within the IJkdijk 2012 experiment: All-in-one Sensor Validation Test (AIO-SVT) [67].

6.3.1. Results of physical modelling

This section contains those results of numerical modelling which have been compared with the results of natural experiment with the aim of demonstration of applicability of finite element modelling (FEM) for prediction tasks. Sensors measuring pore pressure values were selected for comparison with results of numerical experiment.

The model that was constructed by the experts was based on documents and drawings provided by Deltares; finite-element method and finite-element software PLAXIS, which is oriented at studying of soil behaviour.

Two sets of virtual sensors were considered. These two sets correspond to the sensors presented in Figure 2.4. Virtual sensors from one set differ from each other by the distance to the ground surface. Finite-element model with virtual sensors positioning is shown in Figure 6.11.

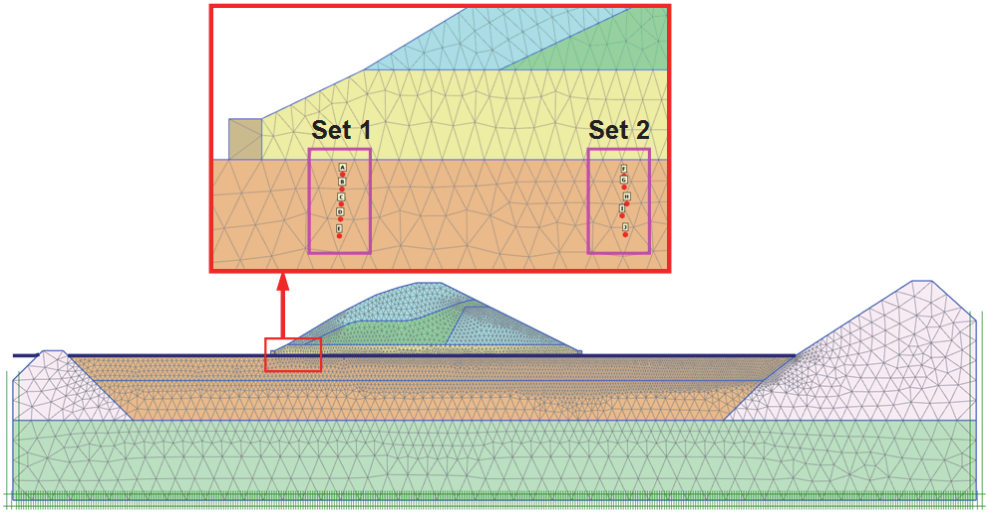

Figure 6.11. Placement of virtual sensors in the West levee.

As soil levees under consideration are lengthy objects at the point of interest, so it was possible to use 2-D model, which describes characteristic cross-section of the object.

The finite-element model of the East Levee is presented in Figure 6.12. 15-nodes 2-D elements were used. Each model has about 300 000 degrees of freedom.

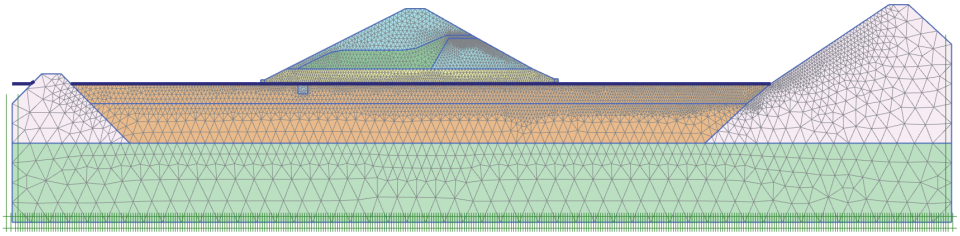

Figure 6.12. The finite-element model of the East Levee.

Water level changing during the experiment is presented in Figure 6.13.

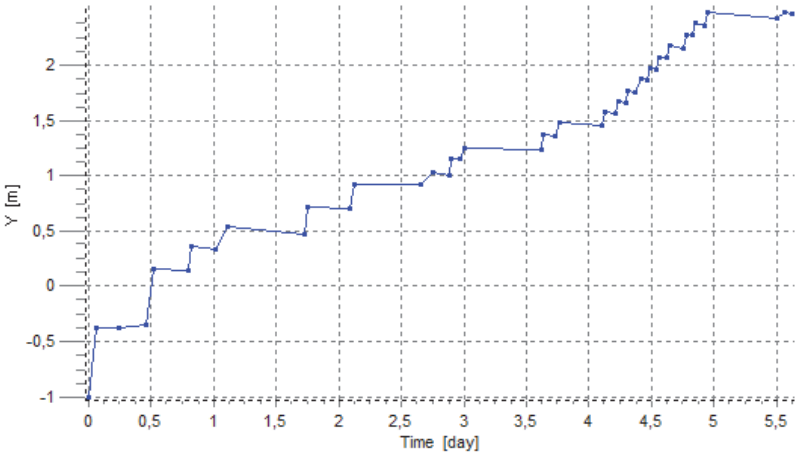

Figure 6.13. Changing of water level in East Levee.

Distribution of pore pressure at different stages of natural experiment is presented in Figure 6.14 - Figure 6.17. It could be seen, that water rising at north side of the levee leads to increasing the value of pore pressure. Also it should be mentioned that high pore pressure front has non-linear shape under levee body and moves from north to south side of the levee during the experiment.

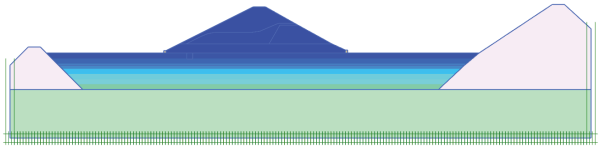

Figure 6.14. Distribution of pore pressure at initial state.

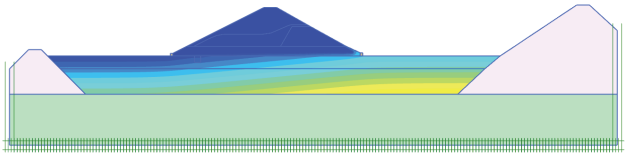

Figure 6.15. Distribution of pore pressure (the water head is 1.6 m).

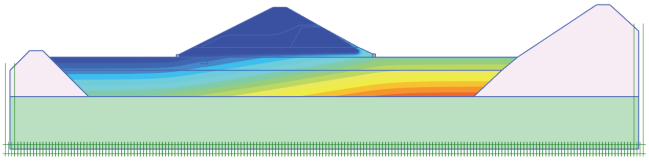

Figure 6.16. Distribution of pore pressure (the water head is 2.8 m).

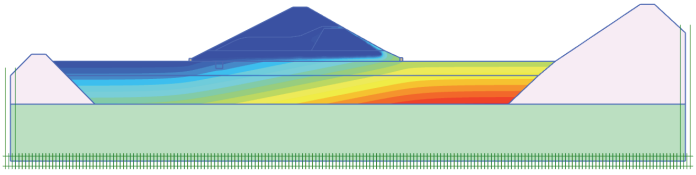

Figure 6.17. Distribution of pore pressure (the water head is 3.4 m).

Distribution of pore pressure which arises at two sets of virtual sensors is shown in Figure 6.18. It is clearly seen that pore pressure values in virtual sensors increase with increasing of depth. Also it increases with moving away from external side of levee.

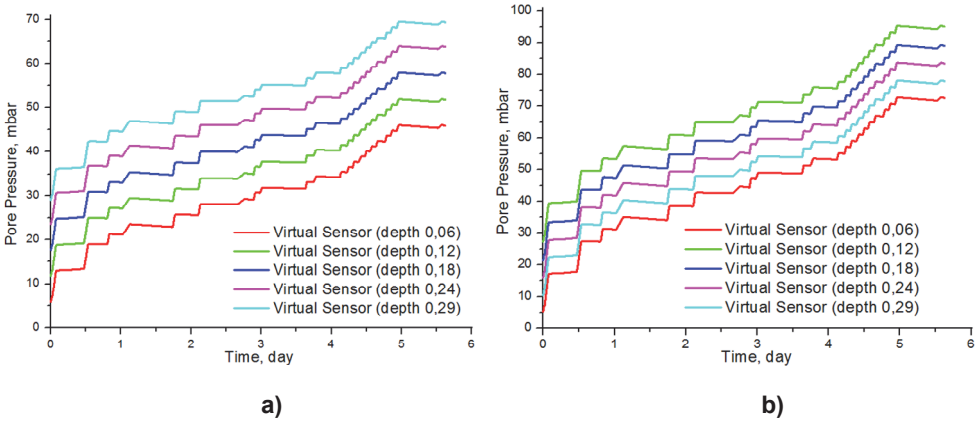

Figure 6.18. (**a**) Pore pressure in set 1 of virtual sensors. (**b**) Pore pressure in set 2 of virtual sensors.

6.3.2. Comparison of virtual and real measurements for the East levee

Figure 6.19 shows comparison between results produced by the Virtual Model developed by Siemens LLC and measurements collected from the Alert Solutions sensors. The Virtual Model simulates behaviour of one cross-section taking into account that soil properties in all cross-sections are the same. The first virtual sensors are marked as AS 213-217, the second set - AS 218-222.

Each step in time series reflects the increase of water level inside the levee. Small shifts between steps for real and virtual measurements are caused by not precise dates in the initial logbook provided by the organizers of the experiment.

For both sensors behaviour look similar till some point in the middle of Figure 6.19 (depends on evaluation of expert). Deviation between real sensor measurements and modelled values can be used for identification of anomaly by visual inspection or using data processing methods [71].

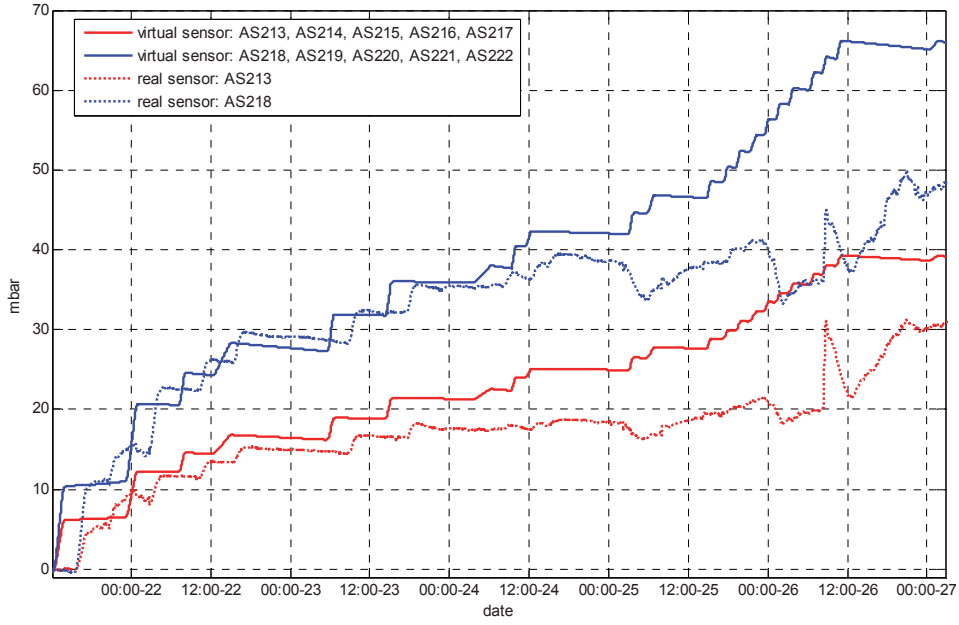

Figure 6.19. East levee: comparison of virtual sensors (solid line) and real sensors (dotted line), AS 213 (red) and AS 218 (blue). X axis: date in format "hh:mm-dd".

6.3.3. Comparison of virtual and real measurements for the West levee

Figure 6.20 shows comparison between Virtual Model and real Alert Solutions sensors. Virtual Model simulates behaviour of one cross-section taking into account that soil properties in all cross-sections are the same. This allows to mark first virtual sensor as SVT 01-03 and second SVT 04-06.

Each step in time series reflects the increase of water level inside the levee. Virtual Model includes also simulation of drainage system activation. Small shifts between steps are caused by not precise dates in the initial logbook provided by the organizers of the experiment.

For both sensors behaviour look similar till some point in the middle of the figure (depends on evaluation of expert). Both figures (Figure 6.19 and Figure 6.20) can be used for visual inspection or used for further data processing – for automatic detection of start of deviation between modelled and real sensors [71].

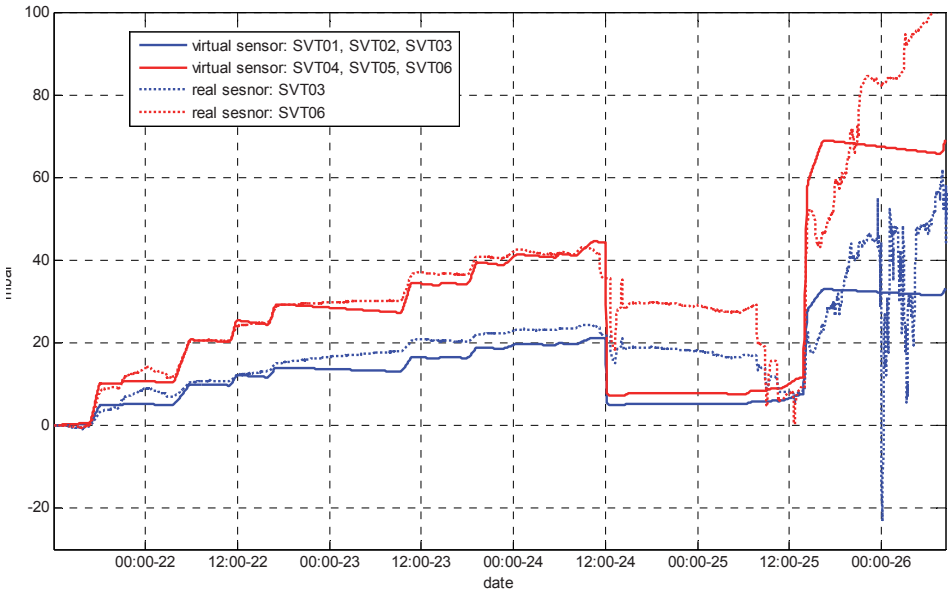

Figure 6.20. West levee: comparison of virtual sensors (solid line) and real sensors (dotted line), SVT 06 – red colour, SVT 03 – blue colour. X axis: date in format "hh:mm-dd".

6.3.4. Anomaly detection on the example of the East levee

Figure 6.21 and Figure 6.22 show comparison of virtual and real sensors for pore pressure and hydraulic head parameters. Small shifts between the same values are represented because of not very precise initial version of the events logbook. Hydraulic head (water level) measurements almost coincide for both of type sensors (virtual and real), for pore pressure values the divergence is presented.

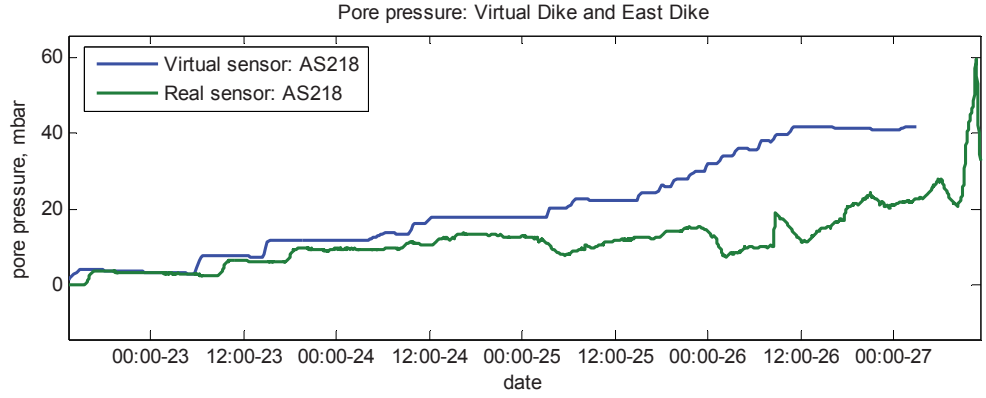

Figure 6.21. East levee: comparison of virtual sensor AS 218 (blue) and real Alert Solutions sensor AS 218 (green). X axis: date in format "hh:mm-dd".

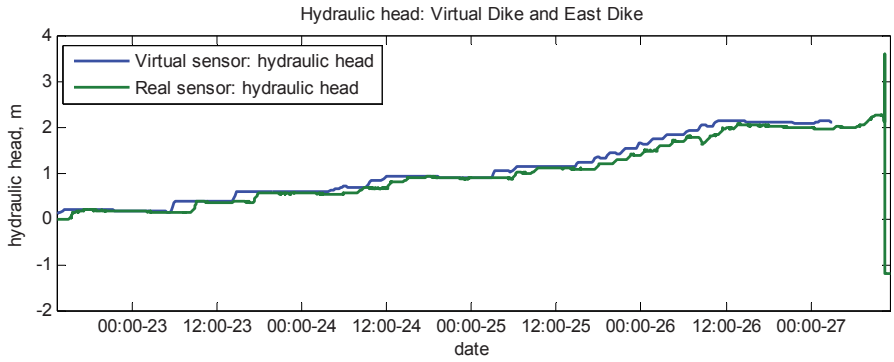

Figure 6.22. East levee: comparison of virtual sensor measuring hydraulic head (blue) and real Deltares sensor (green). X axis: date in format "hh:mm-dd".

The Neural Clouds were trained on pair of virtual sensors (the whole available data set) and tested on real sensors Alert Solutions AS 218 measuring pore pressure and Deltares sensor measuring hydraulic head (the whole available data set).

Figure 6.23 presents clusters constructed on basis of virtual sensors. Black and red points are related to test set: black points are related to clusters related to normal conditions, red point are related to abnormal behaviour.

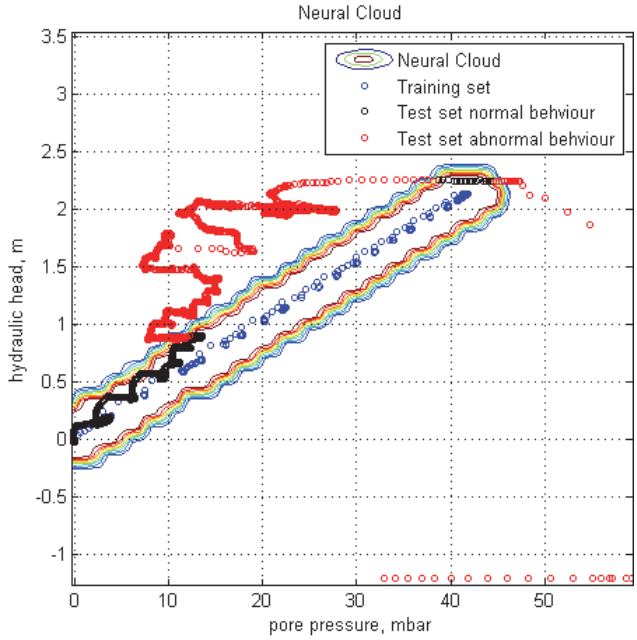

Figure 6.23. East levee: constructed on basis of virtual sensors 2-D clusters of normal behaviour (X axis – pore pressure after air pressure subtraction, Y axis – hydraulic head) and results the real sensor data testing (AS 218 and Deltares hydraulic head): blue circles – training set, black circles – test data related to normal conditions, red circles – data outside clusters related to abnormal behaviour.

In Figure 6.24(b) are presented results of confidence value calculation based on results of clustering presented in the Figure 6.23. The root cause of low confidence value is the difference between real and virtual pore pressure values (Figure 6.24(a)).

First short alarm for 2 data points was identified at 24-Aug-2012 15:06:18 (NL time). Start of the main alarm – 25-Aug-2012 02:06:18.

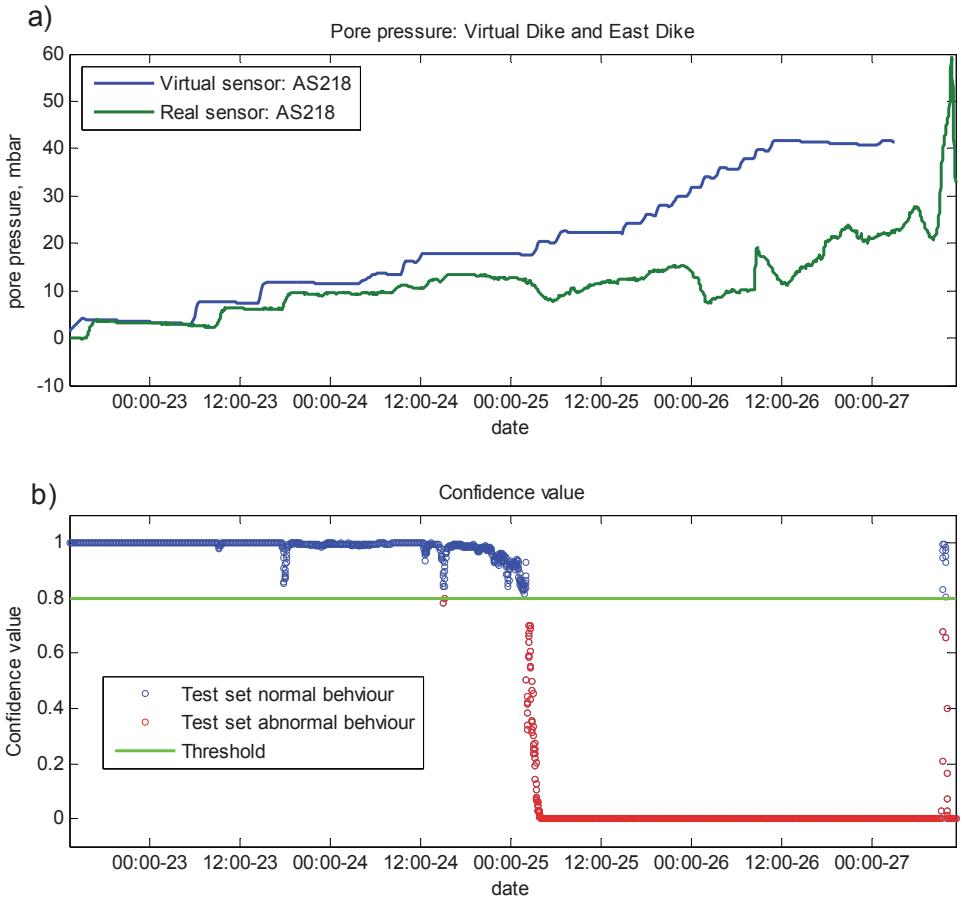

Figure 6.24. East levee. (**a**) Comparison of virtual sensor AS 218 (blue) and real Alert Solutions sensor AS 218 (green). (**b**) Confidence value calculated on basis of clustering presented in Figure 6.23. Blue points are related to normal conditions – higher than selected threshold of 0.8 (green line), red points – alarm situation. X axis: date in format "hh:mm-dd".

6.4. Conclusions

This chapter is dedicated to development of the approach for combination of the data-driven anomaly detection approach with physical modelling and validation of the developed approach (*fifth scientific objective*).

The possible variants of combination are presented. There are two different opportunities: physical model can be used for data generation or for validation of the alarms generated by a data-driven model.

In the first case, the physical model can generate patterns of abnormal behaviour for testing of the developed anomaly detection approach. The physical model can generate normal data if there are no historical measurements but monitoring using data-driven methods has to be started immidiately.

In the second case, the physical model can be used for validation of the generated by the data-driven methods alarms: if the real alarm was detected it is verified. If the false alarm was generated, this can mean that new (previously un-known) state occured, the component should be retrained including these new measurements.

Validation of the developed approach for combination of the anomaly detection approach with physical modelling is presented in the second part of this chapter. Two examples of combination of data-driven methods are presented in this chapter. The first is referred to the *UrbanFlood* project, where the *Virtual Dike* constructed by the University of Amsterdam was used for simulation of a dike similar to the LiveDike (levee protecting Groningen city in the Netherlands) – the same geometry but the material properties have been artificially set weaker. The Virtual Dike simulated change of deformation and strain in several points in conditions of increasing water level. These parameters were used as input for the one-side classifier. The Neural Clouds were able to identify the moment when the stability factor changed the slope angle what can be interpreted as anomaly.

The second example is related to combination of data-driven methods and numerical modelling during the full-scale All-in-One Sensor Validation Test organised in 2012 by the IJkdijk consortium. The physical model developed by Siemens LLC proved to be very accurate [123]. One-side classifier trained on the expected values of water level and virtual sensors (pore pressure) showed in advance divergence from the real sensor measurements (real water level and real pore pressure), that was a sign of developing levee failure.